Transition from persistent to antipersistent correlation in biological systems

Larry S. Liebovitch and Weiming Yang
Center for Complex Systems, Florida Atlantic University, Boca Raton, Florida 33431
(Received 7 April 1997)

Fractal analyses on several noiselike time series from biological experiments reveal transitions from persistent correlation to antipersistent correlation. In this paper, we discuss several simple random walk models which produce such transitions, and therefore are candidates for the mechanisms that may be present in these biological systems. These mechanisms are a correlated fractal random walk that is constrained by a threshold or environmental or inertial forces. We find that persistent correlations for brief time intervals can arise by inertial movement, while for the long time intervals antipersistent correlations can arise from the fact that the natural system is bounded. We also estimate the transition point between these two correlation behaviors. The results agree with the experiment in magnitude. [S1063-651X(97)04710-7]

PACS number(s): 87.10.+e, 47.53.+n, 05.40.+j

I. INTRODUCTION

Many noiselike fluctuations are now thought to be fractal time series [1–5]. Since they are generally correlated and do not satisfy Gaussian statistics, they cannot be characterized by their moments, since these are not defined for such distributions. However, they can be characterized by how the variance depends on the time over which it is measured [6]. The parameter that characterizes how the variance depends on time interval is called the ''Hurst coefficient''; it is related to fractal dimension, and also provides information about correlations. When the Hurst coefficient $H=0.5$, then the values of a time series are uncorrelated with each other. When $0<H<0.5$, then the values of a time series are said to be ''antipersistent'' because increases in the values are more likely to be followed by subsequent decreases, and vice versa. When $0.5<H<1$, then the values of a time series are said to be ''persistent'' because increases in the values are more likely to be followed by subsequent increases and, similarly, decreases are more likely to be followed by subsequent decreases. Because these correlations are fractal, they are present over all time scales.

Recently, fractal analysis has been widely used to investigate noiselike fluctuations in biological systems [1–5]. In this paper, we would like to call attention to a common feature found in the fractal analysis results of several biological experiments done by Churilla *et al.* [1], Collins and De Luca [2], and Treffner and Kelso [3]. Churilla *et al.* recorded the voltage difference across the cell membrane of human *T*-lymphocyte cell lines. Collins and De Luca studied the human postural control system. They measured the time series of human postural sway. Treffner and Kelso studied how normal human adults attempted to balance an aluminum rod which could be held at its pivot (at the bottom), but was constrained to slide on a one-dimensional track of 180 cm in length. A common result of the above experiments is that a transition from persistent to antipersistent correlation was found. Over brief time intervals, the correlation is persistent and the Hurst coefficient H is around 0.8. Over long time intervals, the correlation is antipersistent, and the Hurst coefficient H is about 0.3.

The coincidence of correlation behavior in these experiments suggests that there may exist some common dynamical components in these biological systems which contribute persistent and antipersistent correlations, respectively. The components which contribute persistent correlation dominate in the brief time interval. For the long time interval, other components which contribute antipersistent correlation become dominant. To discuss dynamical properties of fluctuations, it is helpful to analyze the system as an analogy of a random walk process, or a Brownian motion. The persistent correlation may arise from inertial movement. Unlike the ordinary Brownian motion conventionally considered, the effective mass of the ''particle'' in a biological system generally cannot be neglected [7]. Inertial movement can be very important for brief time intervals in biological system. The antipersistent correlation may arise from the fact that the random walk is bounded. In the above experiments, the voltage differences are limited in order to keep the stability of the membrane, the postural sways are limited to a range otherwise that humans cannot stand, and in Treffner's experiment not only is the balancing established in a limited angle range but the track is also of limited length. The bounded system naturally provides an antipersistent correlation for the long time interval.

The paper is organized as follows: in Sec. II we briefly review the theory of fractional Brownian motion and the method of fractal analysis. We compare three different methods of estimating the Hurst coefficient. In Sec. III, we recalculate the Hurst coefficient for the time series from Churilla's experiment by the three methods we discussed in Sec. II. The motivation is to try to characterize the transition from persistent to antipersistent correlation more thoroughly. In Sec. IV, several simple models considering bounded potential or inertial movement are considered. The numerical results on correlation behavior are compared with the results in Sec. III, and we try to illustrate the effect of different dynamical components. Theoretical analyses and numerical calculations on the transition point, at which the correlation changes from persistent to antipersistent, are provided for all the models we discuss. Discussions and conclusions are in Sec. V, where we also estimate the relaxation times of inertial movement for the three experimental systems we mentioned above.

II. FRACTAL ANALYSIS OF TIME SERIES

A. Fractional Brownian motion

By definition, an important property of fractal times series is statistical self-similarity. One of the simplest example is ordinary Brownian motion in one dimension. Consider a particle in fluid with mass m is driven by uncorrelated random force $\eta'(t)$, while a viscous force depending on velocity is also present. We have the Langevin equation.

$$m\ddot{x} = -\gamma\dot{x} + c\,\eta'(t), \tag{1}$$

where $-\gamma\dot{x}$ is the viscous force and c is the random force amplitude. The above equation could also be written

$$\ddot{x} = -\dot{x}/\tau + c\,\eta(t), \tag{2}$$

where $\tau = m/\gamma$ is called the relaxation time and $\eta(t) = \eta'(t)/m$. If the mass of a particle is very small, such that the relaxation time goes to zero, Eq. (1) should be written as

$$\dot{x} = c\,\eta'(t)/\gamma. \tag{3}$$

In this case, the average and the variance of the particle position $x(t)$ satisfy the relations

$$\langle x(t) - x(t_0)\rangle = 0, \quad \langle [x(t) - x(t_0)]^2\rangle = 2D|t - t_0| \tag{4}$$

for any two times t and t_0, where D is called the diffusion coefficient. These relations imply that the process is statistically self-similar. That is, the shape of the motion over times interval $t_1 - t_0$ is proportional to that over interval $t_2 - t_0$. The generalization of the process assumes that the variance satisfies the following relation with $|t - t_0|$:

$$\langle [x(t) - x(t_0)]^2\rangle \sim |t - t_0|^{2H}, \tag{5}$$

which defines a fractional Brownian motion [6]. H is the Hurst coefficient which satisfies $0 < H < 1$. The ordinary Brownian motion corresponds to the special case $H = \frac{1}{2}$, where the values of the time series are uncorrelated with each other. When $H \neq \frac{1}{2}$, the process is properly fractional and has an infinitely long-run correlation. More specifically, when $H < \frac{1}{2}$, an increasing trend in the past implies a decreasing trend in the future, and a decreasing trend in the past implies an increasing trend in the future. Such a correlation is antipersistent. When $H > \frac{1}{2}$, we have a persistent correlation. In this case, an increasing trend in the past implies an increase trend in the future, Conversely a decreasing trend in the past implies, on the average, a continued decrease in the future.

Many people believe that the fractal time series can be analyzed using a framework of fractional Brownian motion, or at least the methods applied to fractional Brownian motion could also be used to characterize some key properties of fractal time series. To develop the tool of analyzing fractional Brownian motion, the first step is to implement the fractional Brownian motion with a computer.

Two computer simulation methods are generally used to generate a fractional Brownian motion. One was developed by Mandelbrot and Wallis [8], which divides each integer time step into n steps for the purpose of approximating the integral and defines the increments of a discrete fractional Brown motion with $0 < H < 1$ as

$$B_H(t) - B_H(t-1) = \frac{1}{\Gamma(H+1/2)} \sum_{i=n(t-M)}^{nt} K\left(t - \frac{i}{n}\right) n^{-1/2} \xi_i, \tag{6}$$

where the kernel K is defined by

$$K(t-t') = \begin{cases} (t-t')^{H-1/2}, & 0 \leqslant t' \leqslant t \\ (t-t')^{H-1/2} - (-t')^{H-1/2}, & t' < 0, \end{cases} \tag{7}$$

and $\{\xi_i\}$ is a set of Gaussian random variables with unit variance and zero mean. Another method was introduced by Voss [9], which he called successive random addition. The starting point is a sequence of positions $X(t_1), X(t_2), \ldots, X(t_N)$ at times $t_1, \ldots, t_N$. We choose $N = 3$ at $t_i = 0$, $\frac{1}{2}$, and 1, and set positions equal to zero. Next, the positions $X(t_1)$, $X(t_2)$, and $X(t_3)$ are given random additions chosen from a Gaussian distribution with zero mean and unit variance. The midpoints of time intervals become additional times at which the positions are estimated by interpolation. Then all positions are given a random addition with zero mean and a reduced variance $\sigma_2^2 = \frac{1}{2}^{2H}$. After n applications of this algorithm we defined the position of the fractional Brownian motion at $(1 + 2^n)$ times. The positions are obtained by the interpolation and random addition process. The variance of the addition in the nth generation of this process is $\sigma_n^2 = \frac{1}{2}^{2Hn}$. Then, introducing a transformation on time $t \to t' = 2^n t$ and on position $X \to X' = 2^{2Hn} X$, we obtain a time series of fractional Brownian motion for t_i from 0 to $2^n + 1$.

The second method is much more efficient for getting a long fractional Brownian motion time series. Thus, in this paper, most of the simulations used the series created by the second method.

B. Rescaled range analysis

In 1951, Hurst introduced rescaled range analysis to study time correlations in annual discharges of the Nile River [10]. That method is well suited for studying the correlation of fractal time series. Consider an increment series $\{x_i\}$ of a fractional Brownian motion. We divide it into $N(T)$ adjacent segments, each of T points. To perform the rescaled range analysis requires that we compute a quantity called R/S for each T. For eliminating possible trend influence, the mean of the nth segment of length T is first computed:

$$\langle x\rangle_{n,T} = \frac{1}{T} \sum_{i=(n-1)T+1}^{nT} x_i. \tag{8}$$

The standard deviation $S_{n,T}$ of the nth segment of length T is defined as

$$S_{n,T} = \left[\left(\frac{1}{T}\right) \sum_{i=(n-1)T+1}^{nT} (x_i - \langle x\rangle_{n,T})^2\right]^{1/2}. \tag{9}$$

For each point i in the time series, we compute

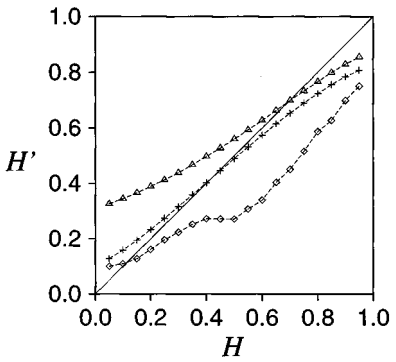

FIG. 1. Estimated Hurst coefficients H' with rescaled range analysis method (Δ), variance analysis method ($+$), and zero-crossing analysis method ($\diamond$) for fractional Brownian motion time series created with successive random addition method for given H.

$$y_{i,n,T}=\sum_{k=(n-1)T+1}^{i}(x_k-\langle x\rangle_{n,T}) \tag{10}$$

for $(n-1)T+1\leqslant i\leqslant nT$. The range $R_{n,T}$ in the nth segment is then computed by subtracting the least value of $y_{i,n,T}$ from the greatest value of $y_{i,n,T}$. We divide the range by the standard deviation to determine the rescaled range, and define an average rescaled range

$$(R/S)_T=\frac{1}{N(T)}\sum_{n=1}^{N(T)}(R_{n,T})/(S_{n,T}). \tag{11}$$

We calculate the rescaled ranges for different time duration T, and the logarithm of $(R/S)_T$ is plotted versus the logarithm of T. The slope of this plot is H, the Hurst coefficient.

To test the method and our computer program quantitatively, we first generated some time series of fractional Brownian motion with a given H by the kernel integral method and by the successive random addition method, then computed the Hurst coefficients and compared them with the predefined value. The result is shown in Fig. 1. For the rescaled range analysis, the Hurst coefficient is overestimated when $H<0.7$, and underestimated when $H>0.7$.

C. Variance analysis

In the variance analysis method we directly calculate the variance of increments $V(t-t_0)$, and determine how the variance diverges with time. Consider a time series of fractal Brownian motion $X(t)$, the variance of increments is given by

$$\begin{aligned}V(t-t_0)&=\langle[X(t)-X(t_0)-\langle X(t)-X(t_0)\rangle]^2\rangle\\&=\langle[X(t)-X(t_0)]^2\rangle-\langle X(t)-X(t_0)\rangle^2,\end{aligned} \tag{12}$$

which by definition diverges with time as

$$V(t-t_0)\sim|t-t_0|^{2H}. \tag{13}$$

Numerical results show the Hurst coefficients determined by this method are the closest to the predefined H (Fig. 1). However, since our testing sequences are much more accurately fractal than real data, some unexpected influences may be introduced when we analyze the real experimental data. The important point is that the analysis directly considers the variance quantity, which is one of the most important properties in the stochastic process and connected with many other physical measurables. Whatever the accuracy of the estimated H is, the dependence of the variance on the time interval provides important information about the process.

D. Zero-crossing analysis

Generally speaking, the time series $\{X_n\}$ from experiment are some scalar observable $X_n=h(\mathbf{Y}_n)$, in which $\mathbf{Y}_n$ are underlying high-dimensional variables. So it is important to introduce methods which directly extract the information of fractal properties from time series. Hereafter we develop a method that uses the zero-crossing property of a fractional Brownian motion.

According to Ref. [11], the distribution $P(T)$ of the first return time T for a fraction Brownian motion satisfies a power law

$$P(T)\sim T^{H-2}, \tag{14}$$

where H is the Hurst coefficient. The first return time is defined by the event

$$X(0)=X(T)=x_0,\quad X(t)<x_0\quad\text{for } 0<t<T$$

or, symmetrically,

$$X(0)=X(T)=x_0,\quad X(t)>x_0\quad\text{for } 0<t<T$$

The discrete versions of the above event are

$$\begin{aligned}&X(0)=x_0,\quad X(1)<x_0,\quad X(2)<x_0,\ldots,\\&\qquad X(T)<x_0\quad\text{and}\quad X(T+1)\geqslant x_0\end{aligned}$$

or

$$\begin{aligned}&X(0)=x_0,\quad X(1)>x_0,\quad X(2)>x_0,\ldots,\\&\qquad X(T)>x_0\quad\text{and}\quad X(T+1)\leqslant x_0.\end{aligned}$$

By the embedding theorem of a dynamical system, we can derive that the distribution of zero crossing is invariant for a generic scalar function h.

Some details of the above analysis should be considered when we proceed to use the zero-crossing analysis. The first is that the finite length of the time series may cause the statistics of the long return times to be characterized with low accuracy. The second is that a power law is established on a continuous motion. The discrete sampling may miss a lot of return events. It will affect the statistics especially for short return times. Hence only the statistics for a medium range of return times is reliable. More specifically, if the sample length is N, the statistics of the return times between 10 and $N/10$ are thought to be the most reliable.

Our numerical test results on the fractional Brownian motion with given H are shown in Fig. 1. The length of the time series is 8192. We measured the slope d of the distribution on a log-log plot between $T=10$ and 1000. The Hurst coefficient measured is $d+2$. The values estimated for H by this method were less accurate than those determined by the other methods. The main reason is that the length of the time

series is too short. We also analyzed time series of lengths up to 32 769. For this longer time series, the estimated values by zero-crossing analysis are better than ones given by the rescaled range analysis, but worse than ones given by the variance analysis. The values computed from these three methods underestimate the value of H when H is near 1. This error is reduced for the variance analysis and the zero-crossing analysis as the length of the time series increases.

The results in Fig. 1 show the comparison of the different methods. The further evaluations of the methods are important and complicated [12]. Here we want to note that, since our test sequences are accurate fractional Brownian motions, we are not certain that we would find the same results when applying these methods to real experimental data. We think that each of these methods may provide a different point of view on the fractal time series. In the following, we will use all three methods to analyze the time series and compare them with the simulating results from the models. Here we would like to note that the zero-crossing analysis needs relatively longer time series to ensure the reliability of its statistics. Although the zero-crossing analysis is invariant under a coordinate transformation, we still use it as a reference tool while the other two methods are more prominent in our discussion, since the experimental time series are generally relatively short.

III. TRANSITION FROM PERSISTENT TO ANTIPERSISTENT

Fractal analysis now has been applied to characterize many time series from biological systems. It is found that a unique Hurst coefficient could not be defined for the entire process. Generally, for the short time interval, the slopes in different analyses all suggest that the Hurst coefficient is larger than 0.5, while, for the longer time interval, the slopes suggest that the coefficient is smaller than 0.5. A Hurst coefficient larger than 0.5 means a persistent behavior, which carries out a superdiffusion which is faster than a normal random walk; and, conversely, a Hurst coefficient smaller than 0.5 means a antipersistent behavior, which carries out an abnormal diffusion which is slower than a normal random walk. Since it is a common property of many biological systems, we think the mechanism of the transition from persistent to antipersistent correlation could be derived from the property of a dynamical system.

First, we would like to detail the description of the transition by using the analysis methods mentioned in Sec. II. As a typical example, we choose data from Churilla *et al.*'s experiment [1], which is a measure of the voltage across the cell membrane of human T-lymphocyte cell line by the whole cell patch clamp technique. The time series consisted of 8192 points sampled at 100 points/s. Since the slope varies for different time intervals, we calculated the local slope and converted it to the corresponding Hurst coefficient for a certain time interval. The result is shown in Fig. 2.

By rescaled range analysis, for a time interval smaller than 1 s, the values of H are between 0.65 and 0.90. For time intervals larger than 10 s, the values of H are around 0.2. The transition point, at which the value of H hits 0.5, is about 4.2 s. Variance analysis presents a slightly different picture. The values of H, beginning from 0.83 for the shortest time interval we have (0.02 s), decrease to around 0 at a time interval of around 5 s. Different from the result of a rescaled range analysis, H is 0.34 for the time interval is 1 s. The transition point from persistent to antipersistent correlation is about 0.45 s, which is about one decade smaller than the one in the rescaled range analysis. The effective analyzing interval range for zero-crossing analysis is 0.1–10 s. The computation result shows the values of H are an average 1 for time interval from 0.1 to 1 s and an average 0.4 for a time interval from 1 to 10 s. The transition point is around 1 s.

We also did the same analyses on other data from Churilla *et al.*'s experiment, and the data from Treffner and Kelso's experiment [3]. A similar behavior was observed. The absolute value of H fluctuated while the feature of a transition from persistent to antipersistent correlation remained. The transition point obtained from the variance analysis was one decade smaller than the one obtained from the result of the rescaled range analysis.

IV. MODELS

A. Bounded correlated random walk

The motivation of our work is to find some simple dynamical models which could illustrate the transition from persistent to antipersistent correlation. There are several possible ways to implement the transition. We first considered a constrained persistent random walk model. Because the biological system is naturally a bounded system, the time series we measured from a biological system carries this property, and we could introduce limitations $X_{\max}$ and $X_{\min}$ in our model. When the particle moves to the boundary of limitation, it is bounced back as if there is a mirror at the boundary. Our first model considered a fractional Brownian motion with mirrors at $X=-M/2$ and $M/2$. In practice, we first created a time series of a free fractional Brownian motion, and then introduced a mirror transformation

$$X(t)\rightarrow X'(t)=\begin{cases} M-X(t), & X(t)>M/2 \\ X(t), & -M/2\leqslant X(t)\leqslant M/2 \\ -M-X(t), & X(t)<-M/2. \end{cases} \tag{15}$$

We did the transformations on the time series many times until all values of $X(t)$ were between $-M/2$ and $M/2$. Figure 3 shows the fractal analysis result for transformed time series of fractional Brownian motion with $H=0.75$ and $M=100$.

The results do show a transition from persistent to antipersistent correlation. The transition point from the variance analysis is also one decade smaller than the ones from the rescaled range analysis. However, the transitions are sharper than those found from the experiment. After the transition, instead of the value of H about 0.2 in the results of fractal analysis on experimental data, the rescaled range and the increment variance of the model's output correspond to $H=0$.

The transition point from persistent to antipersistent could be derived by the following argument: When the particle does not hit the boundaries, the motion of the particle maintains a persistent behavior. The free-moving time between the boundaries determines the magnitude of the transition

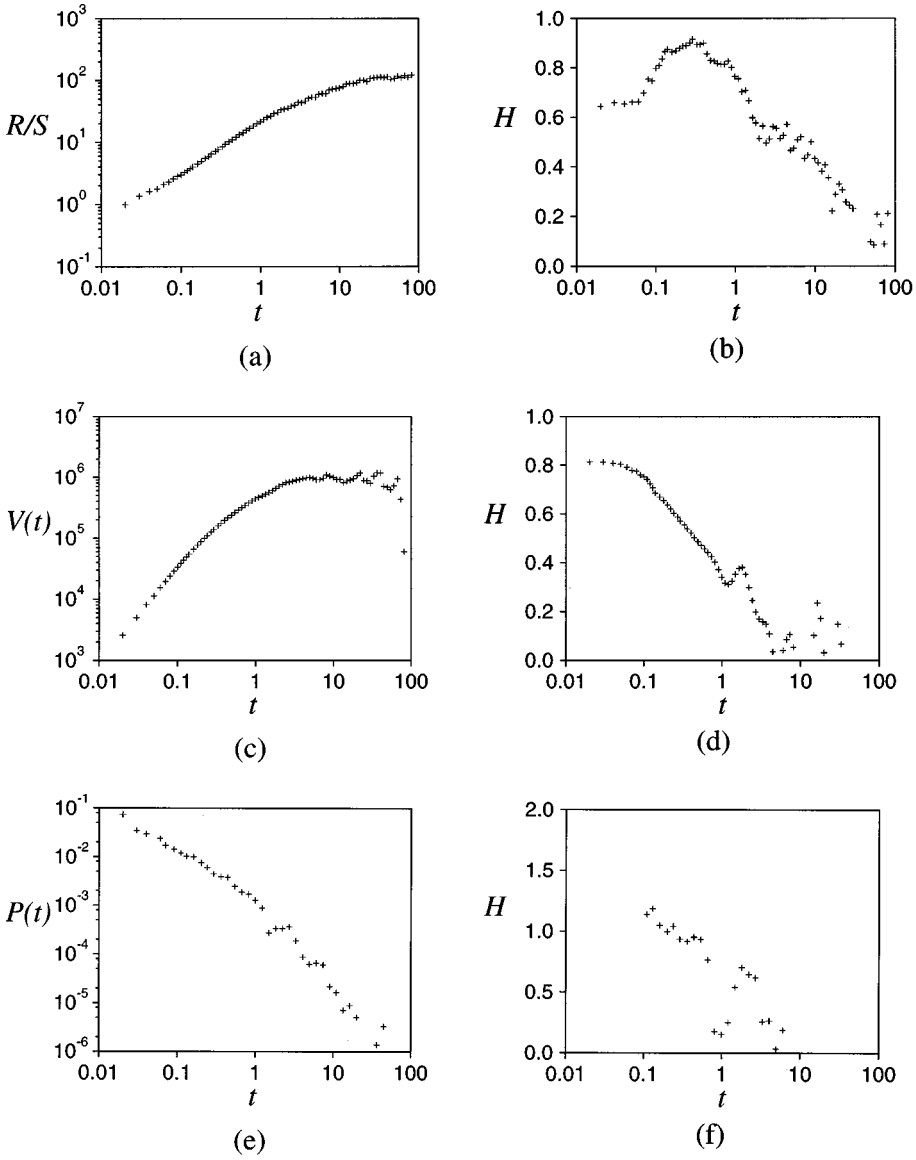

FIG. 2. Results of fractal analyses on the time series of case C in Churilla *et al.*'s experiment [1]. (a) The rescaled range R/S vs the time interval t in a double logarithm coordinate. (b) The coefficient H of the local slope in (a) vs the time interval t. (c) The variance of increment $V(t)$ vs the time interval t in a double logarithm coordinate. (d) The coefficient H derived from the local slope in (c) vs the time interval t. (e) Distribution $P(t)$ of the first return time t in a double logarithm coordinate. (f) The coefficient H derived from the local slope in (e) vs the time interval t which is between 0.1 and 10 s.

point. Suppose the diffusion coefficient of a primary random walk is D; we will have a transition point at approximately

$$T_c = C_m (M/D)^{1/H}, \tag{16}$$

where H is the Hurst coefficient, and C_m is a constant for a given H. Figure 4 shows the numerical result of the transition point for different M/D when the Hurst coefficient is 0.75. The slopes of both lines are $\frac{4}{3}$. For the rescaled range analysis, the value of C_m is about 0.55, while, for the variance analysis, C_m is 0.09. We also calculate dC_m for different Hurst coefficients. It seems C_m is independent of H in this case.

The mirror approximation shows that introducing a constraint on random motion does cause an antipersistent correlation, as we expected. However, the antipersistent correlation in this model is stronger than we have seen in the experiment. We believe that the reason for this difference between experiment and our mirror approximated constrained model is that the mirror's bouncing back virtually introduces an infinitely strong force at the boundary, which does not really exist. To overcome the disagreement between model and experiment, one obvious way is to consider a softer constrained force, e.g., an elastic recovering force, acting on the particle associated with the stochastic force.

To do this, we need to solve the differential equation of motion with a stochastic force which is represented by fractional Brownian noise. We put fractal Brownian noise ξ in Eq. (3) instead of ordinary random noise. When we solve that equation numerically, we use the increment of a fractional Brownian motion instead of a random number chosen from a Gaussian distribution for each integral step. The output of x will be a fractional Brownian motion with same

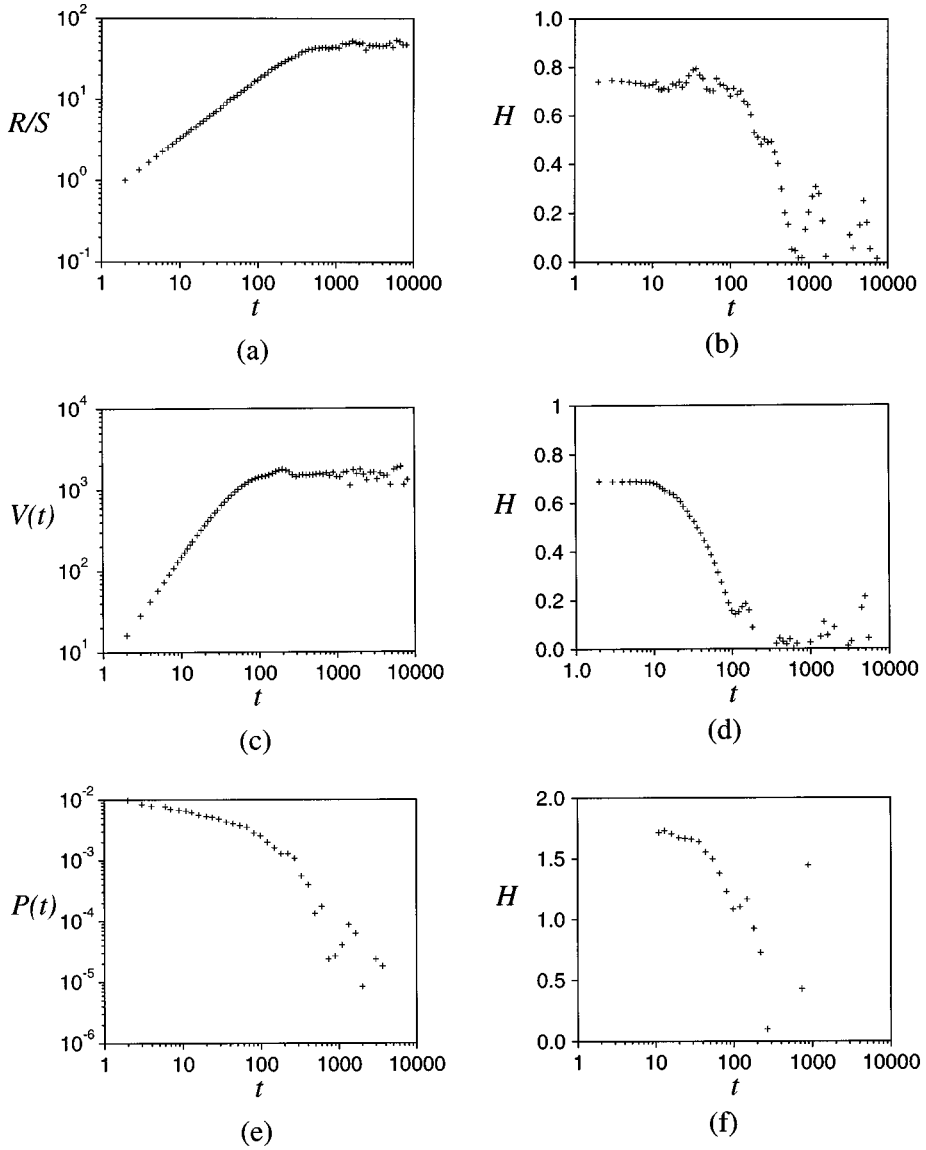

FIG. 3. Results of fractal analyses on the time series of model (15) for $H=0.75$, $M=100$, and $D=1$. (a) The rescaled range R/S vs the time interval t in a double logarithm coordinate. (b) The coefficient H derived from the local slope in (a) vs the time interval t. (c) The variance of increment $V(t)$ vs the time interval t in a double logarithm coordinate. (d) The coefficient H derived from the local slope in (c) vs the time interval t. (e) Distribution $P(t)$ of the first return time t in a double logarithm coordinate. (f) The coefficient H derived from the local slope in (e) vs the time interval t, which is between 10 and 1000 unit times.

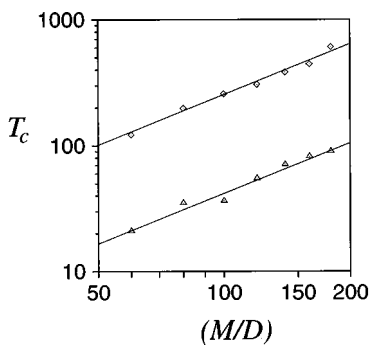

FIG. 4. The transition time T_c by the rescaled range analysis ($\diamond$) and the variance analysis (Δ) for different M/D in model (15). Here $H=0.75$. The equations of the straight lines in figure are $T_c=0.55(M/D)^{4/3}$ and $T_c=0.09(M/D)^{4/3}$.

Hurst coefficient. Next we can add in a elastic recover force $-kx$ in Eq. (3), to obtain

$$\dot{x}=-kx/\gamma+c\xi'(t)/\gamma. \tag{17}$$

The random force $\xi'(t)$ is a fractional Brownian noise.

More specifically, we used a first-order integral method to solve Eq. (17). The key point is assuming that the output of equation $\dot{x}=\xi'(t)$ is a perfect fractional Brownian motion, then

$$\int_t^{t+h}\xi'(t)dt=h^H Y, \tag{18}$$

where Y is chosen progressively from a series of the increments of a fractional Brownian motion with unit variance and zero mean. Thus we have

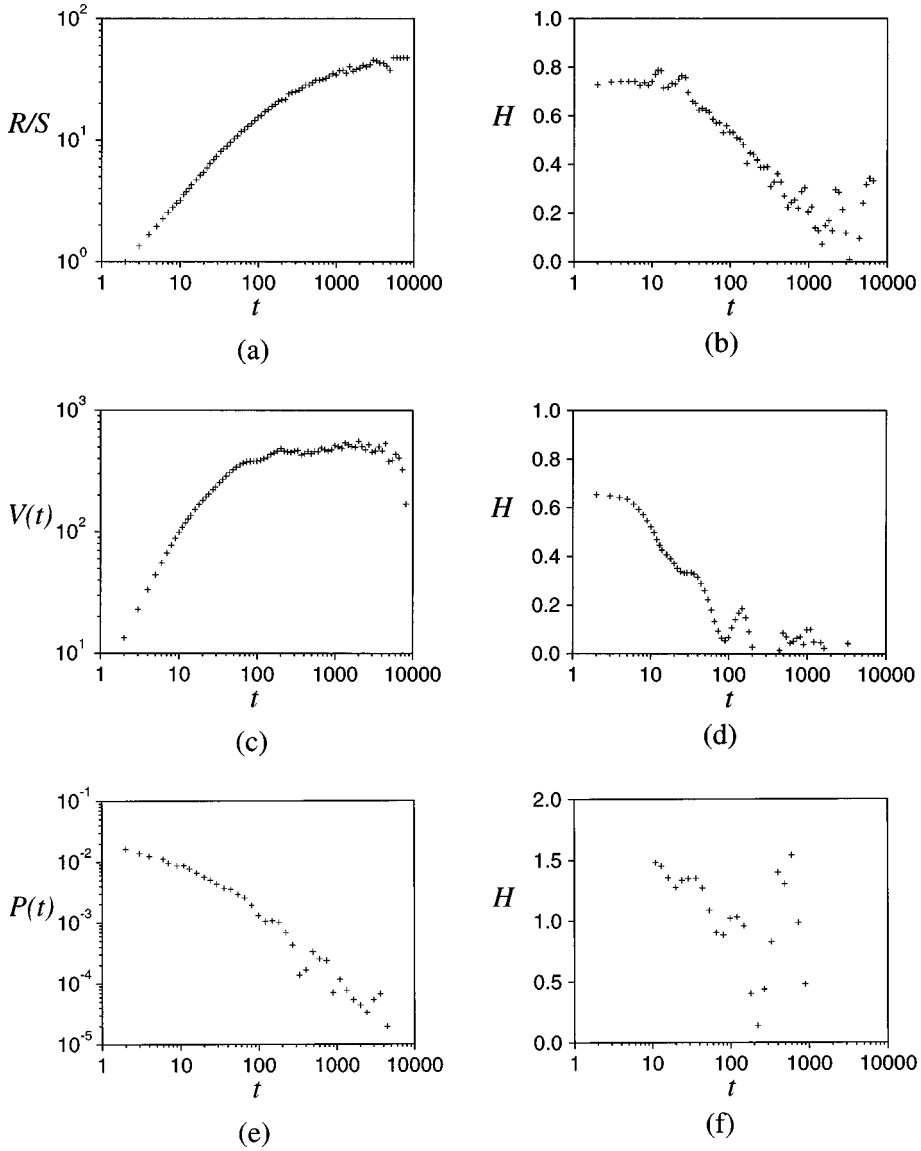

FIG. 5. Results of fractal analyses on the time series of model (17) for $H=0.75$, $k/\gamma=0.06$, and $c/\gamma=1$. (a) The rescaled range R/S vs the time interval t in a double logarithm coordinate. (b) The coefficient H derived from the local slope in (a) vs the time interval t. (c) The variance of increment $V(t)$ vs the time interval t in a double logarithm coordinate. (d) The coefficient H derived from the local slope in (c) vs the time interval t. (e) Distribution $P(t)$ of the first return time t in a double logarithm coordinate. (f) The coefficient H derived from the local slope in (e) vs the time interval t, which is between 10 and 1000 unit times.

$$x(t+\delta t)-x(t)=-kx\,\delta t/\gamma+c(\delta t)^{H}Y/\gamma. \tag{19}$$

The result of the fractal analysis for output time series from Eq. (17) is shown in Fig. 5. The Hurst coefficient of the fractional Brownian noise is chosen to be 0.75. The viscous coefficient γ is 1, the elastic parameter k is 0.06, and the random force amplitude is 1.

The rescaled range analysis of this process presents almost the same behavior as that of the experiment. For long time intervals, the Hurst coefficient goes around 0.3. The only disagreement between the results of the experiment and the model comes from the variance analysis. The transition from persistent to antipersistent correlation seems still to be sharper than the one we have seen in results on experiment data. We also tried a softer force, i.e., $F=-k|x|^{1/2}$. The results are not qualitatively different. The transition is still sharper than that in the result on experimental data with the variance analysis.

Another conclusion from the assumption that $\dot{x}=\xi'(t)$ is that for the output, a perfect fractional Brownian motion, under the transformation $t\rightarrow t'=at$, the random force term is statistically transformed under $\xi'(t)\rightarrow\xi'(t')=\xi'(at)=a^{H-1}\xi'(t)$. This result is important when we discuss the transition point of model (17). Under the transformations $t\rightarrow t'=\gamma k^{-1}t$ and $x\rightarrow x'=c\,\gamma^{H-1}k^{-H}x$, Eq. (17) is scaled to a equation without parameters. That implies a statistical similarity among the systems with different parameters, and the transition point T_c satisfies

$$T_c=C_e\gamma/k, \tag{20}$$

where C_e is a constant for a given H. The numerical result of the transition points is shown in Fig. 6. In Fig. 6(a), we

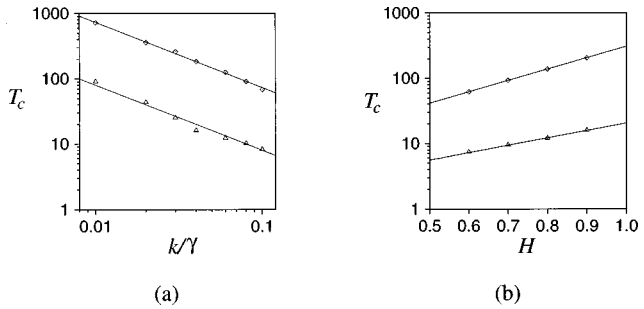

FIG. 6. (a) The transition time T_c by the rescaled range analysis ($\diamond$) and the variance analysis (Δ) for different k/γ in model (17) when $H=0.75$. The equations of the straight lines in the figure are $T_c=7.3/k$ and $T_c=0.8/k$. (b) The transition time T_c by the rescaled range analysis ($\diamond$) and the variance analysis (Δ) for different H in model (17) when $k/\gamma=0.06$. The equations of the straight lines in figure are $T_c=e^{1.73+4H}$ and $T_c=e^{0.42+2.6H}$.

calculate the transition points of model (17) for different k/γ, while the Hurst coefficient of the fractional Brownian noise is 0.75. The slopes of the line in the figure are both -1. C_e is about 7.3 for the result of rescaled range analysis, and about 0.8 for the result of variance analysis. Numerical exploration using different Hurst coefficients [Fig. 6(b)] shows that the value of C_e does depend on the value of H with $C_e \propto a^H$. The equations of the two lines are $\exp(1.73+4H)$ and $\exp(0.42+2.6H)$, respectively, which imply that a is about 55 for the result of rescaled range analysis, and about 13 for the result of variance analysis.

B. Fractional Brownian motion with long relaxation time

Now we consider the problem from another side. We assume the underlying process is an antipersistent fractional Brownian motion, while other physical properties of the system contribute persistent behavior for brief time intervals.

The simplest consideration is the inertial movement of the particle. Unlike the Brownian particle in fluid, the effective mass in a biological system may not be ignored in our observation time scale. This means that the relaxation time of the inertial movement, which equals m/γ, is comparable with the observation time scale, and thus the inertial movement will be observed in the biological experiment. Inertia always tries to keep the particle moving in the same direction, or, in other words, the inertial movement is a persistent movement. Thus we can expect that a persistent correlation could exist, at least when the time interval is smaller than the relaxation time of the inertial movement. To supply the detail, we still need numerical simulations of the equation of motion. In this case, the stochastic differential equation should derive from the Langevin equation. Changing the random force $\eta(t)$ by fractional Brownian noise $\xi(t)$ in Eq. (2), we obtain

$$\ddot{x}=-\dot{x}/\tau+c\xi(t). \tag{21}$$

We apply a first-order integral method, similar to that used in Sec. III to solve the equation numerically:

$$x(t+\delta t)-x(t)=\dot{x}(t)\,\delta t,$$

$$\dot{x}(t+\delta t)-\dot{x}(t)=-\dot{x}(t)\,\delta t/\tau+c(\delta t)^H Y. \tag{22}$$

The fractal analysis result of the output time series when $H=0.25$, $\tau=10$ and $c=1$ is shown in Fig. 7.

This result seems to be the most similar to that of experimental data. The transition in the variance analysis is as smooth as we have seen in experiment. This suggests that the persistent correlations in experiment are provided by some kind of inertial movements.

Now we consider the relation between the transition point and system parameter in our model. The transformation $t\to t'=\tau t$ and $x\to x'=c\tau^{H+1}$ could scale out all parameters in Eq. (21). Hence the statistical similar property implies that we have

$$T_c=C_i\tau, \tag{23}$$

where C_i is a constant for a given H. The numerical result of transition point for different k and $H=0.25$ is shown in Fig. 8(a). The slopes of the line in the figure are both 1. $C_i\approx 36$ for the result of the rescaled range analysis, and $C_i\approx 3.5$ for the result of the variance analysis. C_i also depends on the Hurst coefficient in this case. Numerical simulations on different fractional Brownian noises show that $C_i\propto b^H$, which are shown in Fig. 8(b). The equations of the two lines are $\exp(5.2+2.08H)$ and $\exp(2.56+4.15H)$, which imply that b is about 8 for the rescaled range analysis, and is about 64 for the variance analysis.

V. CONCLUSIONS AND DISCUSSIONS

We studied how the pattern seen in the experimental data of biological systems, that is persistent at short time intervals and antipersistent at long time intervals, could arise from dynamical systems. We find that the pattern in the data could be due to either (1) a persistent correlated random walk ($H>\frac{1}{2}$) that is bounded by a sharp threshold or a softer force at long times ($H<\frac{1}{2}$), or (2) an antipersistent correlated walk at long time intervals ($H<\frac{1}{2}$) strongly driven by inertial term ($H>\frac{1}{2}$) at short times.

Considering that time series in real systems cannot reach infinity and are generally constrained in some definite range, the bounded walk model is quite reasonable. Numerical simulation verifies that the bounded walk presents an antipersistent correlation for the long time intervals. However, a detailed comparison of our fractal analysis between this simple model and the experimental data shows that there are some differences in transition behavior. For the bounded walk with a mirror approximation, the antipersistent correlation is stronger than what we have seen in experiment. The value of H is too low (~ 0), for models with an elastical recover force and an even softer force ($\sim|x|^{1/2}$). The transition from large H to low H is not as smooth at present in the variance analysis of the data. We also numerically investigated a model which considers inertial force and elastical recover force simultaneously. We also are struck by the fact that the transition from persistent to antipersistent correlation is quicker than we expected. We think that the constrained phenomena in biological systems may not be illustrated by any form of recovering force. A possible explanation is that

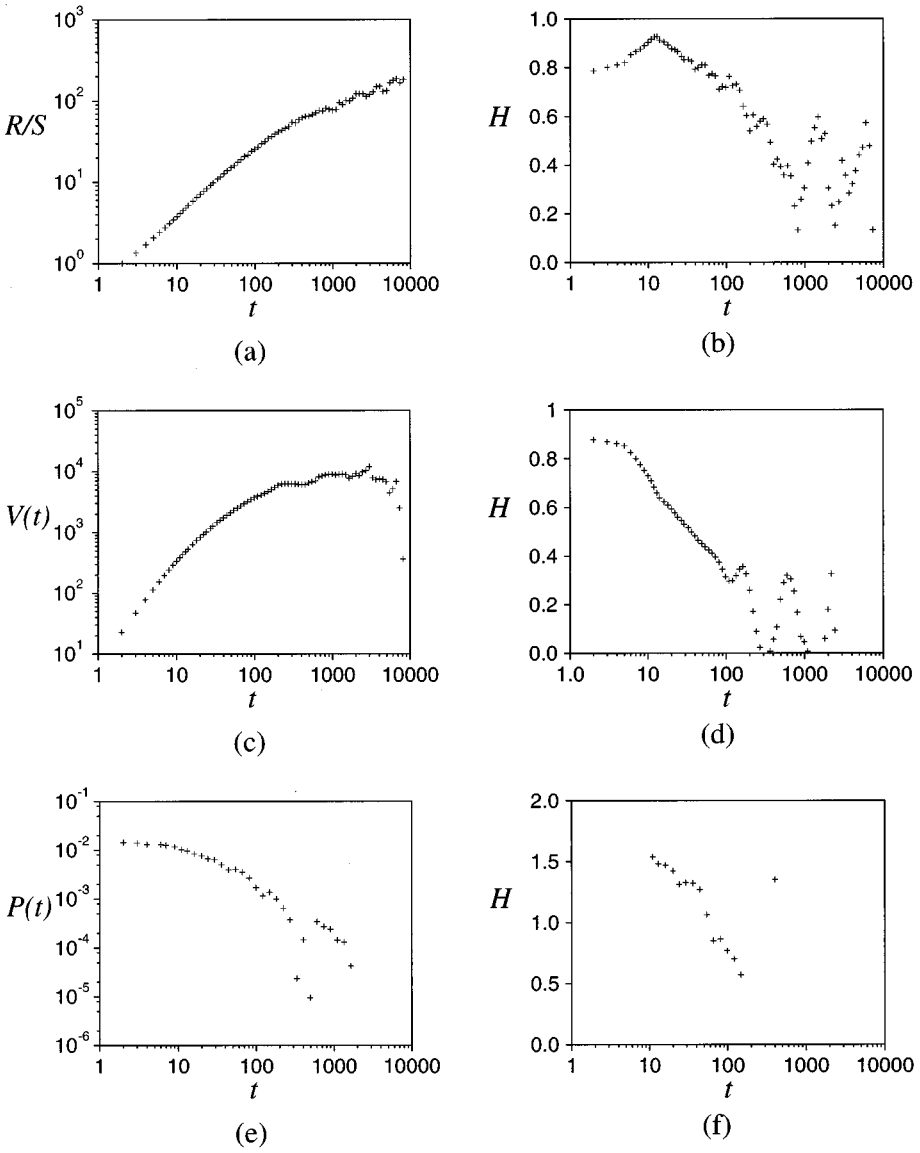

FIG. 7. Results of fractal analyses on the time series of model (21) for $H=0.25$, $\tau=10$, and $c=1$. (a) The rescaled range R/S vs the time interval t in a double logarithm coordinate. (b) The coefficient H derived from the local slope in (a) vs the time interval t. (c) The variance of increment $V(t)$ vs the time interval t in a double logarithm coordinate. (d) The coefficient H derived from the local slope in (c) vs the time interval t. (e) Distribution $P(t)$ of the first return time t in a double logarithm coordinate. (f) The coefficient H derived from the local slope in (e) vs the time interval t, which is between 10 and 1000 unit times.

since there exist many meta steady states in biological systems, the walk is an analogy of a random walk in a random environment. Sinai [13] found that a random environment actually constrains the random walk. For the particular model he discussed it is found that in n steps the particle cannot go farther than $(\ln n)^2$. This result corresponds to that the slope of R/S is $2/\ln n$. For $n>55$, the correlation becomes antipersistent. We will discuss this consideration further in a future paper [14].

To compare the fractal analysis result between model and experiment, the value of the transition point is the most important quantity when we discuss the transition from antipersistent correlation to persistent correlation. The critical reason is that the value of the transition point is strongly connected with the physical parameters, as we discussed in Sec. IV. We derived that the transition point for the model considering the inertial movement depends linearly on the

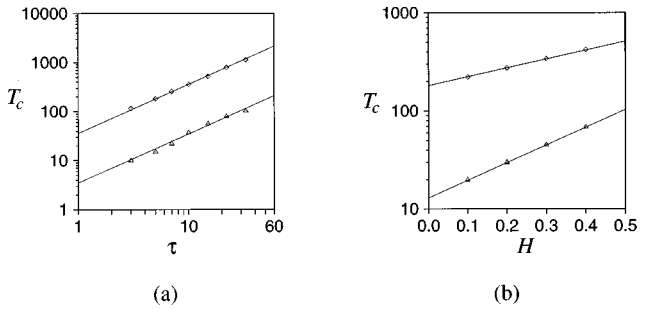

FIG. 8. (a) The transition time T_c by the rescaled range analysis ($\diamond$) and the variance analysis (Δ) for different τ in model (21) when $H=0.25$. The equations of the straight lines in figure are $T_c=36\tau$ and $T_c=3.5\tau$. (b) The transition time T_c by the rescaled range analysis ($\diamond$) and the variance analysis (Δ) for different H in model (21) when $\tau=10$. The equations of the straight lines in figure are $T_c=e^{5.2+2.08H}$ and $T_c=e^{2.56+4.15H}$.

relaxation time τ. For systems similar to Churilla *et al.*'s experiment, it is found that the time scale for changes of voltage in the cell is around 100 ms [15]. We assume this time scale is of the same magnitude as the relaxation time of the process. Since the transition point from a variance analysis is about 3.5τ, and that from a rescaled range analysis is about 36τ, the predicted transition points are consistent with what we found in Sec. III. The postural sway system and Treffner's system are relatively more complicated. We assume the human reaction time is the relaxation time of these two systems, such that the transition point as a result of variance analysis should be around 0.8 s, which is in agreement with the experiment in magnitude. Hence we conclude that persistent correlations in experiment are due to the inertial movement.

Another important phenomenon we found in our work is that, when we employ different fractal analysis methods on the same time series, the transition points from the persistent correlation to the antipersistent correlation are different. This implies that different methods present different results on correlation, and most likely reveal different kinds of correlations. When we investigate the correlation properties of a time series, it is important to apply several different fractal analysis methods in order to characterize the fractal properties more thoroughly. From the theoretical point of view, there are two interesting questions waiting for answers. The first one is why the transition points are different. Our numerical results show the transition point in a rescaled range analysis are always 6–14 times larger than one we obtained in a variance analysis. The second question concerns the dependence on H of C_e and C_i, which is connected with a specific model. It includes why it is an exponential dependence, and why a and b in our two models show opposite trends on different transition points as a result of variance analysis and rescaled range analysis, recalling that a in the variance analysis is four times larger than it is in the rescaled range analysis, while b in the rescaled range analysis is eight times larger than b in the variance analysis. For the model of fractional Brownian motion with elastic recovery force, H is considered to be larger than 0.5, while for the model of fractional Brownian with inertial force, H is supposed to be smaller than 0.5. The difference in the transition point in different fractal analysis methods will be the smallest when $H=0.5$.

ACKNOWLEDGMENTS

This work was supported in part by NIH Grant No. EY6234. The authors thank Dr. M. Ding and Dr. A. T. Todorov for helpful discussions.

[1] A. M. Churilla, Ann. Biomed. Eng. **24**, 99 (1996).
[2] J. J. Collins and C. J. De Luca, Phys. Rev. Lett. **73**, 764 (1994).
[3] P. Treffner and S. Kelso, *in Studies in Perceptions and Action: Proceedings of the International Conference on Perception and Action,* edited by B. G. Bardy, R. J. Bootsma, and Y. Guiard (Erlbaum, Mahwah, NJ, 1995).
[4] I. Giaever and C. R. Keese, Physica D **38**, 128 (1989); R. B. King and S. A. Roger, Circ. Res. **65**, 578 (1989); C. K. Peng *et al.*, Nature (London) **356**, 168 (1992); B. Hoop, H. Kazemi, and L. Liebovitch, CHAOS **3**, 27 (1993); C. K. Peng *et al.*, Phys. Rev. Lett. **70**, 1343 (1993); R. A. Nogueira *et al.*, Braz. J. Med. Biol. Res. **28**, 491 (1995); J. B. Bassingthwaighte and B. Hoop *et al.*, CHAOS **5**, 609 (1995); J. M. Hausdorff *et al.*, J. Appl. Physiol. **80**, 1448 (1996).
[5] J. B. Bassingthwaighte, L. S. Liebovitch, and B. J. West, *Fractal Physiology* (Oxford, New York, 1994).
[6] J. Feder, *Fractals* (Plenum, New York, 1988).
[7] C. C. Chow and J. J. Collins, Phys. Rev. E **52**, 907 (1995).
[8] B. B. Mandelbrot and J. R. Wallis, Water Resour. Res. **5**, 228 (1969); **5**, 242 (1969); **5**, 260 (1969).
[9] R. F. Voss, in *Fundamental Algorithms in Computer Graphics*, edited by R. A. Earnshaw (Springer-Verlag, Berlin, 1985).
[10] H. E. Hurst, Trans. Am. Soc. Civ. Eng. **116**, 770 (1951); H. E. Hurst *et al.*, *Long-Term Storage: An Experimental Study* (Constable, London, 1965).
[11] M. Ding and W. Yang, Phys. Rev. E **52**, 207 (1995).
[12] J. B. Bassingthwaighte and G. M. Raymond, Ann. Biomed. Eng. **22**, 432 (1994); **23**, 491 (1995).
[13] Ya. G. Sinai, Theor. Probab. Appl. **27**, 256 (1982).
[14] L. S. Liebovitch and W. Yang (unpublished).
[15] R. Benz, O. Fröhlich, P. Läuger, and M. Montal, Biochim. Biophys. Acta **394**, 323 (1975); E. Neher and A. Marty, Proc. Natl. Acad. Sci. USA **79**, 6712 (1982).